

JET CROSS SECTIONS AND JET SHAPES IN PHOTOPRODUCTION AT HERA[†]

C. GLASMAN, REPRESENTING THE H1 AND ZEUS COLLABORATIONS

*DESY - F1, Notkestrasse 85,
22603 Hamburg, Germany*

Studies on the structure of the photon are presented by means of the extraction of a leading order effective parton distribution in the photon and measurements of inclusive jet differential cross sections in photoproduction. Measurements of the internal structure of jets have been performed and are also presented as a function of the transverse energy and pseudorapidity of the jets.

The main source of jets at HERA^a comes from collisions between protons and quasi-real photons ($Q^2 \approx 0$, where Q^2 is the virtuality of the photon) emitted by the electron beam (photoproduction). At lowest order QCD, two hard scattering processes contribute to jet production¹: the resolved process, in which a parton from the photon interacts with a parton from the proton, producing two jets in the final state; and the direct process, in which the photon interacts pointlike with a parton from the proton, also producing two jets in the final state.

The study of high- p_T jet photoproduction provides tests of QCD and allows to probe the structure of the photon. In perturbative QCD the cross section for jet production is given by

$$\frac{d^4\sigma}{dydx_\gamma dx_p d\cos\theta^*} \propto \frac{f_{\gamma/e}}{y} \sum_{ij} \frac{f_{i/\gamma}}{x_\gamma} \frac{f_{j/p}}{x_p} |M_{ij}(\cos\theta^*)|^2 \quad (1)$$

where $f_{\gamma/e}$ is the flux of photons from the electron approximated by the Weizsäcker-Williams formula; $y = E_\gamma/E_e$ is the inelasticity parameter; $f_{i/\gamma}$ ($f_{j/p}$) are the parton densities in the photon^b (proton), extracted from the data; $x_\gamma = E_i/E_\gamma$ ($x_p = E_j/E_p$) is the fractional momentum of the incoming parton from the photon (proton); and $|M_{ij}(\cos\theta^*)|^2$ are the QCD matrix elements for the parton-parton scattering.

There are two approaches to the study of the structure of the photon. One approach is to extract directly from the data an effective parton distribution in the photon. The second approach is to measure jet cross sections

[†]Talk given at the "Meeting on Deep Inelastic Scattering", Madrid, Spain, June 1997.

^aHERA provides collisions between positrons of energy $E_e = 27.5$ GeV and protons of energy $E_p = 820$ GeV.

^bThe resolved and direct processes are included in $f_{i/\gamma}$.

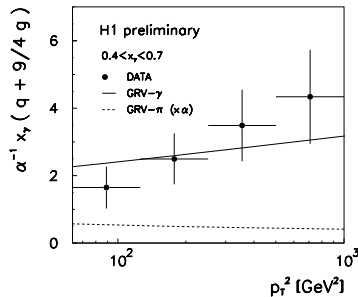


Figure 1: Leading order effective parton distribution in the photon.

that can be calculated theoretically which then provide a testing ground for parametrisations of the photon structure function.

The method² to extract an effective parton distribution in the photon is based on the use of the leading order (LO) matrix elements for the subprocesses with gluon exchange, which give the dominant contribution to the jet cross section in resolved processes for the kinematic regime studied. Then, the quark and gluon densities are combined into an effective parton distribution:

$$\sum [f_{q/\gamma}(x_\gamma, p_T^2) + f_{\bar{q}/\gamma}(x_\gamma, p_T^2)] + \frac{9}{4} f_{g/\gamma}(x_\gamma, p_T^2) \quad (2)$$

A LO effective parton distribution in the photon was extracted³ by unfolding the double differential dijet cross section as a function of the average transverse energy of the two jets with highest transverse energy and of the fraction of the photon's energy participating in the production of the two highest-transverse-energy jets (x_γ). The measurement was performed using a fixed cone algorithm⁴ in the pseudorapidity^c (η) – azimuth (φ) plane with $R = 0.7$ in the kinematic range $0.2 < y < 0.83$ and $Q^2 < 4 \text{ GeV}^2$. Figure 1 shows the extracted effective parton distribution as a function of the scale p_T (the transverse momentum of the parton). The data exhibit an increase with the scale p_T which is compatible with the logarithmic increase predicted by QCD⁵ (i.e., the anomalous^d component of the photon structure function). The predictions using the GRV-LO⁶ parametrisations of the parton densities in the photon and the pion are also shown in figure 1. The data disfavour a purely hadronic behaviour and are compatible with the prediction which includes the anomalous component.

^cThe pseudorapidity is defined as $\eta = -\ln(\tan \frac{\theta}{2})$, where the polar angle θ is taken with respect to the proton beam direction.

^dThe anomalous component of the photon reflects the contribution of quarks from the pointlike coupling of the photon to a quark-antiquark pair.

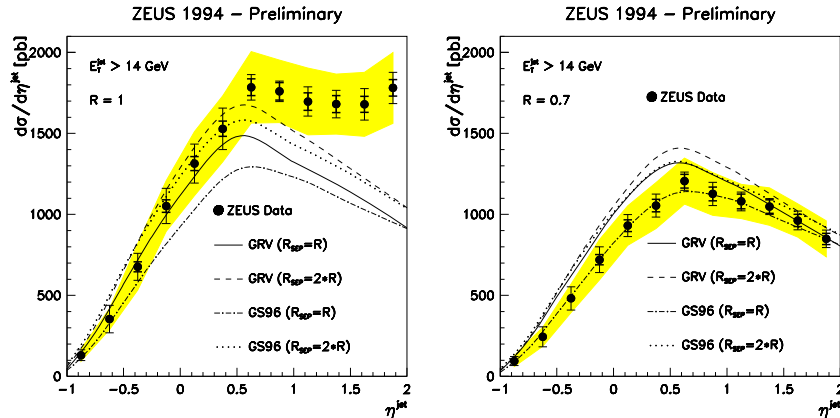


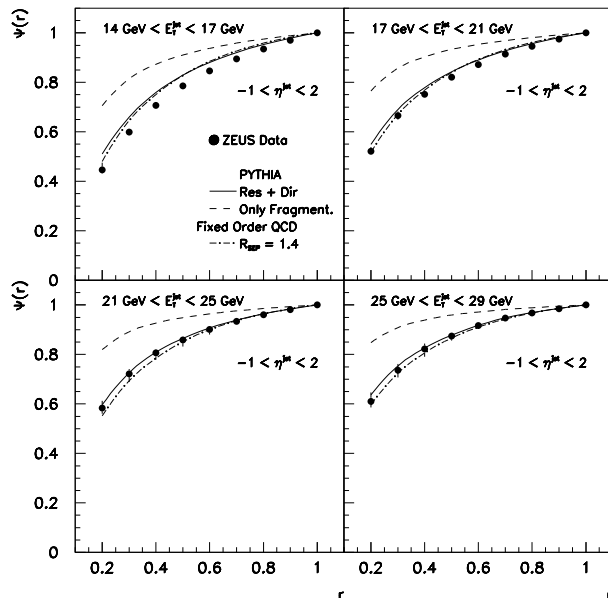
Figure 2: Inclusive jet differential cross sections.

The second approach to the study of the photon structure function is to provide measurements of differential jet cross sections at high jet transverse energies, where the proton parton densities are constrained by other measurements, and, therefore, are sensitive to the photon structure function.

Figure 2 shows the measurements of the inclusive jet differential cross sections for jets searched with an iterative cone algorithm⁴ as a function of the jet pseudorapidity (η^{jet}) for jets with transverse energy satisfying $E_T^{jet} > 14$ GeV. The measurements were performed in the kinematic region given by $0.2 < y < 0.85$ and $Q^2 \leq 4$ GeV², and for two cone radii: $R = 0.7$ and 1. The behaviour of the cross section as a function of η^{jet} in the region $\eta^{jet} > 1$ is very different for the two cone radii: it is flat for $R = 1$ whereas it decreases as η^{jet} increases for $R = 0.7$. It is noted that a given E_T^{jet} threshold for jets defined with $R = 0.7$ corresponds to a higher E_T^{jet} threshold for jets with $R = 1$ and this fact may account for part of the observed differences.

Next-to-leading order (NLO) QCD calculations⁷ are compared to the measurements in figure 2 using two different parametrisations of the photon structure function: GRV-HO⁸ and GS96⁹, and two values of^e R_{SEP} . The CTEQ4M¹¹ proton parton densities have been used in all cases. For forward jets with $R = 1$ an excess of the measurements with respect to the calculations is observed. This discrepancy is attributed to a possible contribution from non-perturbative effects (e.g., the so-called “underlying event”), which are not included in the theoretical calculations. This contribution gets largely reduced by decreasing the size of the cone since the transverse energy density

^eThe parameter¹⁰ R_{SEP} is introduced into the NLO calculations in order to simulate the experimental jet algorithm by adjusting the minimum distance in $\eta - \varphi$ at which two partons are no longer merged into a single jet.


 Figure 3: Jet shapes: E_T^{jet} dependence.

inside the cone of the jet due to the underlying event is expected to be roughly proportional to the area covered by the cone. A very good agreement between data and NLO calculations is observed for measurements performed using a cone radius of $R = 0.7$ for the entire η^{jet} range measured. The predictions using GRV-HO and GS96 show differences which are of the order of the largest systematic uncertainty of the measurements. Thus, these measurements exhibit a sensitivity to the parton densities in the photon and can be used in quantitative studies.

To study the internal structure of the jets, the jet shape $\psi(r)$ has been used. $\psi(r)$ is defined as the average fraction of the jet's transverse energy that lies inside an inner cone of radius r , concentric with the jet defining cone¹⁰:

$$\psi(r) = \frac{1}{N_{jets}} \sum_{jets} \frac{E_T(r)}{E_T(r=R)} \quad (3)$$

where $E_T(r)$ is the transverse energy within the inner cone and N_{jets} is the total number of jets in the sample. By definition, $\psi(r=R) = 1$. The jet shape is affected by fragmentation and gluon radiation. However, at sufficiently high E_T^{jet} the most important contribution is predicted to come from gluon emission off the primary parton.

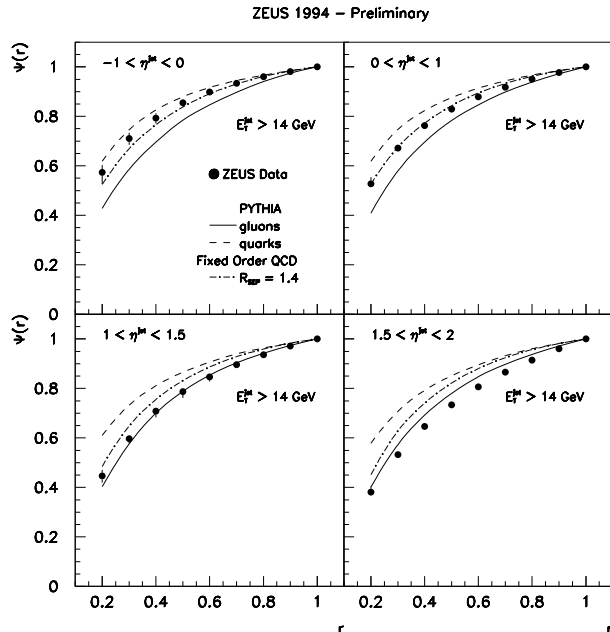


Figure 4: Jet shapes: η^{jet} dependence.

Figure 3 shows the measured jet shapes $\psi(r)$ as a function of the inner cone radius r using a cone algorithm with radius $R = 1$ for jets with $-1 < \eta^{jet} < 2$ and in four regions of E_T^{jet} . As a jet becomes narrower, the value of $\psi(r)$ increases for a fixed value of r . It is observed (see figure 3) that the jets become narrower as E_T^{jet} increases. For comparison, the predictions from leading-logarithm parton-shower Monte Carlo calculations as implemented in the PYTHIA program¹² for resolved plus direct processes are shown in the same figure. For $E_T^{jet} > 17$ GeV the predictions reproduce reasonably well the data. In the lowest- E_T^{jet} region small differences between data and the predictions are observed. PYTHIA including resolved plus direct processes but without initial and final state parton radiation predicts jet shapes which are too narrow in each region of E_T^{jet} . These comparisons show that parton radiation is the dominant mechanism responsible for the jet shape in the whole range of E_T^{jet} studied.

The η^{jet} dependence of the jet shape is presented in figure 4. It is observed that the jets become broader as η^{jet} increases. Perturbative QCD predicts that gluon jets are broader than quark jets as a consequence of the fact that the gluon-gluon is larger than the quark-gluon coupling strength. The predictions of PYTHIA for quark and gluon jets are shown in figure 4. The data go from being dominated by quark jets in the final state ($\eta^{jet} < 0$) to being dominated

by gluon jets ($\eta^{jet} > 1$). Therefore, the broadening of the measured jet shapes as η^{jet} increases is consistent with an increase of the fraction of gluon jets.

Lowest non-trivial-order QCD calculations¹³ of the jet shapes are compared to the measurements in figures 3 and 4. The fixed-order QCD calculations with a common value of $R_{SEP} = 1.4$ reproduce reasonably well the measured jet shapes in the region $E_T^{jet} > 17$ GeV and in the region $-1 < \eta^{jet} < 1$.

The results on photoproduction of jets presented here constitute a step forward towards testing QCD and the extraction of the photon parton densities.

Acknowledgments

I would like to thank the organizers of the conference for an enriching atmosphere and their warm hospitality.

References

1. J.F. Owens, *Phys. Rev. D* **21**, 1980 (54).
2. B.L. Combridge and C.J. Maxwell, *Nucl. Phys. B* **239**, 1984 (429).
3. T. Ebert, representing the H1 Collab., to appear in Proceedings of the “5th International Workshop on Deep Inelastic Scattering and QCD”.
4. CDF Collab., F. Abe et al., *Phys. Rev. D* **45**, 1992 (1448); J. Huth et al., Proceedings of the 1990 DPF Summer Study on High Energy Physics, Snowmass, Colorado, edited by E.L. Berger (World Scientific, Singapore, 1992) p. 134.
5. E. Witten, *Nucl. Phys. B* **120**, 1977 (189).
6. M. Glück, E. Reya and A. Vogt, *Z. Phys. C* **53**, 1992 (127) and *Z. Phys. C* **53**, 1992 (651).
7. M. Klasen and G. Kramer, private communication; “Photoproduction of Jets at HERA in Next-to-Leading Order QCD”, M. Klasen, Ph.D. thesis, DESY-96-204.
8. M. Glück, E. Reya and A. Vogt, *Phys. Rev. D* **46**, 1992 (1973).
9. L.E. Gordon and J.K. Storrow, *Nucl. Phys. B* **489**, 1997 (405).
10. S.D. Ellis, Z. Kunszt and D.E. Soper, *Phys. Rev. Lett.* **69**, 1992 (3615).
11. H.L. Lai et al., *Phys. Rev. D* **55**, 1997 (1280).
12. H.-U. Bengtsson and T. Sjöstrand, *Comp. Phys. Comm.* **46**, 1987 (43); T. Sjöstrand, *Comp. Phys. Comm.* **82**, 1994 (74).
13. G. Kramer and S.G. Salesch, *Phys. Lett. B* **317**, 1993 (218), *Phys. Lett. B* **333**, 1994 (519); M. Klasen and G. Kramer, *Phys. Rev. D* **56** (1997) 2702.